Introducing Improved Loading Assumptions into Analytical Pavement Models Based on Measured Contact Stresses of Tires

Paper Submitted to the International Conference on Accelerated Pavement Testing
Reno, NV, 1999.
Paper Number: CS5-3

Ronald BLAB
Institute of Transportation Studies
University of California, Berkeley
Richmond Field Station
1353 S.46th Street, Bldg. 452
Richmond, CA 94804
Phone: (510) 231 9469
Fax: (510)231 9589
rblab@its.berkeley.edu

ABSTRACT

In spring 1997, three-dimensional (3D) contact stresses occurring between the road surface and three tire types (pneumatic bias ply, radial, and wide base) were assessed by means of the South African Vehicle Road Surface Pressure Transducer Array (VRSPTA) device. Measurements were performed under different load and tire inflation pressure conditions at relatively low speed ranges ("creep speed"). This paper gives a brief description of the VRSPTA device and the test series performed. The results of a comprehensive statistical study on tire geometry and measured contact stresses of the tire imprints are described. Based on this study, regression functions are introduced to estimate both forces and average contact stresses occurring at the tire center and tire edge. Proposals are presented to utilize these regression functions for improved tire load models for pavement analysis. The paper also describes a software program that was developed to transform the space-time dependent 3D measurements of the VRSPTA device to a space only force/stress pattern representing the actual contact stress state at the tire-pavement surface, based on a least-square method optimized for the best fit of the measured and computed (transposed) vertical loads. The software allows users to develop a library of 3D tire stress distributions from any VRSPTA test data. The resulting library may be used for analytical pavement models.

Keywords: **pavement design, pavement/tire interaction, pavement loading, measured contact stresses, Vehicle Road Surface Pressure Transducer Array (VRSPTA).**

Introducing Improved Loading Assumptions into Analytical Pavement Models Based on Measured Contact Stresses of Tires

Paper Submitted to the International Conference on Accelerated Pavement Testing
Reno, NV, 1999.
Paper Number: CS5-3

Ronald BLAB

Institute of Transportation Studies
University of California, Berkeley
Richmond Field Station
1353 S.46th Street, Bldg. 452
Richmond, CA 94804
Phone: (510) 231 9469
Fax: (510) 231 9589
rblab@its.berkeley.edu

INTRODUCTION

Currently used design methods for road pavements employ rather simple assumptions to model contact stresses between the tire and pavement surface. The usual load model for pavement design is a circular, uniform vertical stress equal to the tire inflation pressure. This model may be applicable when distress of the pavement structure at a distance from the surface is considered (St. Venant´s principle), but is highly insufficient to explain surface-related distress, which is more and more becoming the dominant distress mode of modern roads. In recent years, two key forms of failure have been observed at the surface of pavements: surface initiated wheel path cracking and rutting of asphalt concrete (AC) layers. Given that these failure mechanisms occur near the surface of the pavement, a more accurate modeling of the 3D tire/pavement contact stresses is essential.

Prior work has shown that these contact stresses are highly non-uniformly distributed and that considerable differences exist among different types of tires. With the Vehicle-Road Surface Pressure Transducer Array (VRSPTA) (*De Beer 1994*), an effective method has been developed for the measurement of the tire/pavement contact stresses. This information should be utilized for advanced analysis and design of pavements.

This paper describes briefly the test plan of 3D tire contact stress measurements performed with three different tire types used for Accelerated Pavement Testing (APT) with the Heavy Vehicle Simulator (HVS) and compares the effects of different load and inflation pressure conditions on the tire contact stresses identified by statistical data analysis. Based on these findings, a concept for a more advanced load model is developed. A software program is presented to analyze automatically 3D Stress-in-Motion (SIM) measurements obtained from the VRSPTA and to transform them into a corresponding pattern of stresses or forces that can be processed by pavement analysis programs.

TIRE CONTACT STRESS MEASUREMENTS

This paper concentrates on the measurements of three dimensional (3D) tire/pavement contact stress distributions carried out for several pneumatic bias (or cross ply), radial, and wide base type tires used for Accelerated Pavement Testing (APT) at the Pavement Research Center at the University of California, Berkeley (UCB). These 3D contact stress measurements were conducted by means of the Vehicle-Road Surface Pressure Transducer Array (VRSPTA), which was developed by the Division of Roads and Transportation Technology, CSIR, Pretoria, and which is extensively described elsewhere (*De Beer 1994; De Beer 1995a and 1995b*). The tests were made utilizing the Heavy Vehicle Simulator (CAL–HVS1) of the California Department of Transportation (Caltrans) at UCB during February 1997. Test results are reported by De Beer and Fisher (*1997*), but a detailed analysis of the measurements was outside the scope of their report. Some further descriptions of test facilities and equipment used are given there.

The VRSPTA SIM MK II system (hereafter referred to as “VRSPTA”) used in this study consists of 1041 flat-topped, cone-shaped hollow steel pins mounted in 51 rows on a 0.05 m thick steel base plate. Twenty pins mounted in the center row are instrumented with strain gauges forming 20 small tri-axial load cells transversely distributed across the base plate. The remaining pins are supporting pins of equal shape, contact area and stiffness (rigidity) in all directions as the instrumented pins. The VRSPTA is set within a steel frame and embedded such that its surface is flush with the pavement surface. Thus, the stresses (loads) imposed on each tri-axial load cell pin across the contact patch of a passing tire are measured directly and then computed during data post-processing. It therefore gauges the “Stress-in-Motion” (SIM) and quantifies the contact stresses between the passing tire and the pavement surface. Vertical, transverse (or lateral) and longitudinal forces (loads) are recorded from the array of instrumented pins in real time at a fixed sampling rate. A schematic layout of the VRSPTA is given in Figure 1.

The accuracy to measure the actual contact stresses between tire and pavement surface is mainly determined by the following two factors:

- the effective stiffness of the VRSPTA
- the effective friction between VRSPTA and the tire.

Its effective stiffness certainly affects the distribution obtained for both vertical and horizontal stresses/loads and should therefore be in the same order of magnitude as that of the pavement structure considered. This condition is not valid in particular for asphalt concrete (AC) layers at elevated temperatures. Furthermore, effective friction between tire and VRSPTA surface has a dominant effect on the stresses obtained. The surface friction of the

VRSPTA was tested with the TRL (Transport Research Laboratory, UK) Pendulum Skid Resistance Tester and was found to be consistent with a road surface with a “good” skid resistance under dry conditions. This represents a condition where the horizontal forces between tire and VRSPTA can be considered as being relatively close to the their maximum (*De Beer* et al. *1997*).

There are two other shortcomings to acknowledge: The relatively slow (creep) speed of only 3 m/s at which the tests were performed does not represent traffic and loading conditions of free moving vehicles. Furthermore, the given distance between the 3D load cells in the array in the lateral direction introduces some additional errors in the measurements due to the tread pattern of the tire, which can vary up to 65 percent along the tire circumference. Given that the VRSPTA measures the load increments in a 0.017-m line across the tire width, the accuracy is directly influenced by the quantity of rubber in contact with the instrumented pins.

Although some errors are encountered with the measurements, they are believed to represent a clear improvement over the classical assumption of a vertical uniformly distributed circular load equal to the tire pressure with no horizontal components used commonly to define pavement loading.

The extensive study at the Pavement Research Center at UCB included tests using following tire types:

- Goodyear, Bias Ply, 10.00 – 20, Load Range G, SuperHiMiler
  rated 5,630 Ibs (25,5 kN) at 100 PSI (690 kPa) as dual tire
- Goodyear, G159A, 11R22.5, Load Range G, radial tire
  rated 5,470 Ibs (24,8 kN) at 100 PSI (690 kPa) as dual tire
- Goodyear, G425/65R22.5, Load Range J (wide base) as single tire
  rated 10,500 Ibs (47,6 kN) at 110 PSI (760 kPa) or 9,790 Ibs (44,4 kN) at 100 PSI (690 kPa)

For the particular SIM study, a used bias type tire was utilized; both the radial and wide based tire were new. The various VRSPTA test matrices for the tire types used for analysis in this paper are given in Table 1 (p. 11) and 2 (p. 11). For each tire inflation and load level, three repeated measurements were performed and recorded; 222 test runs altogether. It should be noted that CAL–HVS1 loads indicated in each matrix had to be increased by 6 kN from the target loads actually planned for the study because of a malfunction of the CAL–HVS1 static load scale (a hydraulic gauge), that was discovered for different reasons only after the VRSPTA tests (*De Beer* et al. *1997*).

The VRSPTA measures simultaneously the following stresses and stores each of them separately in a file:

- The vertical contact stress ? zz (positive in the downward Z direction)
- The lateral or transverse stress ? zy across the contact area (positive in the Y direction of the VRSPTA, i.e. from pin 1 to 21)
- The lateral or transverse stress ? zx across the contact area (positive in the moving or X direction of the passing wheel)

The sampling rate of 150 Hz for a total of 256 samples for each channel (representing one of the three stress directions) chosen for all test runs was considered to be appropriate for the average speed of 0.3 m/s. Hence, for the 222 runs analyzed in this study approximately 32.3 Mbytes of data had to be processed and evaluated.

MODELING TIRE GEOMETRY AND CONTACT STRESS

By means of a software program developed to analyze SIM data and described in more detail in a following section, some basic statistics are studied first. Among other features, the software offers the opportunity to determine tire geometry (width, length, contact area, etc.) directly from the data of any SIM measurement recorded by the VRSPTA.

Tire Width to Length Ratio

Because of the high lateral tire stiffness, the width *w* of the tire imprints measured is approximately constant and relatively independent of inflation pressure and loading conditions for each of the tire types tested. Table 3 (p. 12) summarizes mean tire width *w*, standard error, and standard deviation calculated for the analyzed sample size *n* of each of three different tire types. Excluded are 9 measurements each conducted under a very low tire inflation

pressure of only 220 kPa with both the bias ply and radial tire, which simulates a flat tire and is therefore rather unusual for normal operation conditions.

For all tire types, the calculated standard deviation is in the range of only ± 0.015 m (or 3-7% of the mean tire width) – within the accuracy range of the SIM device itself. (The pins have a lateral distance to each other of 0.017 m.) The influence of tire inflation pressure and tire loading on the actual tire width is therefore negligible and for each tire type a constant width *w* given in Table 3 (p. 12) can be used for modeling tire imprints of the three given tire types. In general the imprint width *w* can be assumed to be equal to the width of the tire tread area of a given tire type.

In order to illustrate the very different longitudinal stiffness behavior of each of the three tire types tested, the mean ratio of the width and length of their imprint as a function of both the applied vertical tire load F_z and tire inflation pressure p_i are plotted in Figures 2 and 3.

Both bias ply and radial tire imprints show a fairly small range for the mean width to length ratio (0.55-0.65). The deviation around the mean ratio, which is not indicated in Figures 2 and 3, is relatively high. However, all the values measured for bias ply and radial tires are much less then 1. By keeping in mind that tire width approximately stays constant, the assumption of a circular load geometry used in most of today's pavement design calculations is insufficient with respect to conventional tire types. Consequently, a rectangular load geometry is recommended.

While the mean width of the wide base tire imprints is approximately 60% higher than those of the bias ply and the radial tire (see Table 3 p. 12), its mean length is – depending strongly on inflation pressure and loading –10 to 45% lower. This results in a mean ratio of tire width to length that is well above 1 for low loads and decreases rapidly below 1 when the load increases. This ratio only deviates slightly from 1 for increasing inflation pressure conditions. In the rated load and inflation pressure ranges, the mean tire imprint width-to-length ratio of the wide base tire is about 1 (i.e., square imprint). For wide base tires used within their rated loading and tire pressure ranges, square or circular loads can be assumed to idealize tire contact pressure in theoretical pavement models. However, for relatively thick and stiff pavement layers, the load geometry may be less important for the primary response calculated at their bottom but nevertheless may affect the amount and direction of the principal (tensile) stresses and strains (which in most distress models are related to fatigue cracking).

Average Vertical Contact Stress

Most existing methods of quantifying the vertical contact stress for pavement design are based on the rather simple approach of measuring the contact area using the tire imprint and dividing the applied vertical tire load F_z by this area to calculate the average vertical contact stress *q*. By then assuming a circular load symmetry, the associated load radius can easily be determined. However, that load radius has no correlation to the actual geometry of the tire imprint. In many pavement design methods, this average vertical contact stress is further assumed to be nearly equal to the inflation pressure p_i in the "cold" (not operated) truck tire.

Considering sampling rate (frequency), test speed, and the effective area of each instrumented pin of the VRSPTA, the total tire imprint area (including contact and non-contact area between the tread) can be determined. By dividing it by the applied vertical load the average vertical contact stress *q* was calculated for each SIM measurement. Figure 4 shows a boxplot of the q/p_i ratio drawn against the inflation pressure p_i. In general, a boxplot shows a measure of the location (median – bold line), a measure of dispersion (the interquartile range – upper and lower quartiles joined by vertical lines to produce the box), and the presence of possible outliers (vertical lines drawn up from the upper quartile to the most extreme data point that is within a distance of 1.5 of the interquartile range). A boxplot gives an indication of the symmetry or skewness of the distribution.

According to Figure 4, all tire types show the same tendency of decreasing *q* to p_i ratios for higher tire inflation pressures. For the bias ply and radial tire the q - p_i ratio is higher than one only in relatively low inflation pressure ranges and always decreases mostly below one for rated inflation pressures and higher. For wide base tires the *q* to p_i ratio is almost always lower than 1.

The relatively large dispersion of the calculated *q* to p_i ratios within one load range indicates a sensitivity of the calculated average contact pressure not only to tire inflation pressure, but also to the applied tire load. This fact is not taken into account by any recent publication dealing with SIM data analysis (e.g., *de Beer*, et al. *1997*,

Groenendijk, et al. *1997*). Regression analysis shows a good correlation for the following bivariant linear function which can be used in a first approach to calculate the average vertical contact stress q as a function of the actual applied vertical load and the tire inflation pressure:

$$q = k_1 + k_2 p_i + k_3 F_z \quad (1)$$

with

q = average vertical tire contact stress [kPa] F_z = applied vertical tire load [kN]
p_i = tire inflation pressure [kPa] $k_{1,2,3}$ = regression constants

Table 4 (p. 12) gives the regression constants $k_{1,2,3}$ together with the corresponding R-squared values (R^2), which indicate the level of fit for the regression function used and the standard error of the average contact stress estimated for each tire type. The constants of the regression function represent a 50% reliability that the contact stress calculated will not underestimate the actual tire contact pressure. Statistical tests proved the assumption of a normal distribution over these mean values, which allows higher levels of reliability to be derived by taking into account the standard deviation of both the constants and the variables of the regression function. Hence, the coefficients $k_{1,2,3}$ for reliability levels of 80, 90, and 95% can be calculated. They are also summarized in Table 4. The numbers given in Table 4 indicate, as expected, that the higher the reliability percentile value, the higher the vertical contact stress to be used for pavement design purposes. Higher levels of reliability reduce the chances of assuming deficient contact stresses in the design calculations but are associated with potentially overestimating them.

In most cases, even with reliability values of 90 or 95%, the estimated average tire contact pressure is lower than the value of the given inflation pressure. That indicates that the most common approach for load assumptions in pavement analysis (to equal the tire inflation pressure to the contact stress of a uniformly distributed load) overestimates the average vertical stresses actually measured under a tire. But as the vertical contact stresses are non uniformly distributed and stress peaks occur that are 1.5 to 3 times higher than the calculated average vertical stress even under tires operated with rated tire inflation pressure and rated loads, this rather conservative assumption may be justified.

Average Tire Edge and Tire Center Stress

All SIM results with the VRSPTA device show, almost independent from the tire type tested, the clear trend that the higher the applied vertical load of the tire the higher the vertical contact stresses at the tire edge. The measurements further indicate that the tire loading does not strongly affect the development of the vertical contact stresses towards the tire center. The contact stresses at the tire center are primarily influenced by the actual tire inflation pressure. These significant effects have already been demonstrated by earlier SIM measurements and were described by various researchers, some of whom could postulate them purely from a theoretical approach (e.g., *de Beer 1997, Yap 1988*). For pavement design purposes, it is therefore important to distinguish between the different loading conditions across the tire width and the resulting different types of contact stress patterns.

In order to quantify these effects in more detail, each of the tire imprints measured was divided into two edge zones of 20% each and a center zone covering the remaining 60% of the whole tire width. From the SIM record, the SIM Analysis software automatically calculates the vertical tire edge load F_e as well as the vertical tire center load F_c by integrating over the individual loads measured on each instrumented pin from the VRSPTA device at both edge zones and the center zone. Subsequently, the average contact stress at the tire edge q_e and the average contact stress at the tire center q_c is computed. Therefore, the effect of load and contact stress distribution between tire center and tire edge can be studied comprehensively and reliably for the three tested tire types based on the large amount of data collected in this study.

In order to take into account the different loading conditions at the tire edge and the tire center for improved load modeling in pavement design when only the total applied vertical tire load F_z is known, two tire load distribution factors a_e and a_c are introduced. These distribution factors are defined as the ratio between the vertical tire edge load F_e or the vertical tire center load F_c, respectively, and the total applied vertical tire load F_z :

$$\left.\begin{aligned} a_e &= \frac{F_e}{F_z} \\ a_c &= \frac{F_c}{F_z} \end{aligned}\right\} \quad \text{where } a_e + a_c = 1 \tag{2a–c}$$

As the sum of factors a_e and a_c must be 1, a simple tire load distribution factor a can be introduced, which itself is defined as the ratio between the center and the edge load distribution factor. This load distribution factor a may now be used to calculate a_e and a_c in order to derive both the vertical tire edge and tire center load from the total applied vertical load:

$$\left.\begin{aligned} a_e &= \frac{1}{1+a} \\ a_c &= 1-\frac{1}{1+a} \end{aligned}\right\} \quad \text{where} \quad a = \frac{a_c}{a_e} \tag{2d–f}$$

where in Equation (2a-f)

a_e = tire edge load ratio
a_c = tire center load ratio
a = tire load distribution factor
F_z = applied vertical tire load [kN]
F_c = vertical tire center load [kN]
F_e = vertical tire edge load [kN]

Accordingly, the tire load distribution factor a defined above was determined for all SIM measurements performed with the three tire types tested in this study. By means of regression analysis, the influence of the tire inflation pressure p_i and the applied vertical tire load F_z on the factor a was investigated. From all different regression functions tested, again a simple bivariant linear function shows the best fit. The fit seems sufficiently good to be used to estimate the load distribution factor a by facilitating following equation:

$$a = k_1 + k_2\ p_i + k_1\ F_z \tag{3}$$

Further regression analyses were performed on the values computed for the average tire center contact stresses q_c and the average tire edge contact stresses q_e, respectively, by linking them to either one or both of the known parameters: tire inflation pressure p_i, and applied vertical tire load F_z. Contradicting similar studies reported elsewhere, the calculated average tire center contact stress was found to be not solely influenced by the tire inflation pressure but also by the vertical tire load. Hence, following regression function can be used to estimate q_c:

$$q_c = k_1 + k_2\ p_i + k_3 F_z \tag{4}$$

In the case of contact stress development at the tire edges, analysis of the measurements verify the assumption that these stresses are controlled predominantly by the applied vertical tire load. The following relationship, based on a quadratic regression function, gives the best fit to estimate q_c:

$$q_e = k_1 + k_2\ F_z + k_3 F_z^2 \tag{5}$$

where in Equation (3–5)

a = tire load distribution factor
p_i = tire inflation pressure [kPa]
F_z = applied vertical tire load [kN]
q_c = average tire center contact stress [kPa]
q_e = average tire edge contact stress [kPa]
$k_{1,2,3}$ = regression constants

In Tables 5–7 (pp. 12-13), regression constants and statistics including: the estimate for the constants k_1 to k_3; the standard error; as well as the lower and upper 95% confidence limits for these estimates and the R-squared values (R^2) of the regression functions given in Equation 3–5, are summarized for each tire type separately.

All regressions show a good fit with R^2 values between 0.64 and 0.92. Also, the standard errors for the constants k_2 of the linear term and k_3 of the quadratic term are generally low. Only the standard error of k_1, which represents the constant term in each of the regression functions, and which shifts the function along the y axis, is sometimes remarkably high. That means all measurements follow the trend of the regarding regression function very well, but depending on the chosen level of confidence, the function itself varies significantly in the vertical direction.

Figure 5 illustrates the results of the regression analysis obtained for the tire load distribution factor a. This factor a is plotted against the applied vertical load F_z for all three tire types (wide base, radial, and bias ply tire) for different tire inflation values p_i. In the cases of the radial and the wide base tires, if the applied load increases the load shifts from the tire center to the tire edge independent of the actual inflation pressure. The opposite occurs when the bias ply tire is loaded. This effect can be explained by the more rigid tire wall and the more flexible tire tread of the bias ply tires, as opposed to the flexible wall and rigid tread zones of both the radial and the wide base tires. The relatively high flexibility of the tread area in combination with the rigid wall of the bias ply tire also contributes to the higher sensitivity of its load distribution factor a to the actual tire inflation pressure. Generally, for the bias ply tire and the radial tire types the tire inflation pressure has a higher influence on the load distribution between tire edge and tire center then the vertical tire loading, while for the wide base tire the α value is predominantly influenced by the load.

For the rated load and inflation pressure ranges, the α-values for both the radial and the bias ply tire are less then 1, corresponding to a higher tire edge to center load ratio. When the wide base tire is operated in rated ranges, α is greater then 2, which indicates a lower loading rate at the edge compared to the center for this tire.

In Figure 6, the regression functions obtained for the average tire center contact stress q_c are plotted for each tire type as function of the applied vertical tire load F_z for different inflation pressure levels p_i. In case of the bias ply tire type, the average tire center contact stress q_c increases rapidly under increasing loading and inflation pressure conditions, while the radial tire type is less sensitive to the applied tire load but still very sensitive to the actual inflation pressure. The average tire center contact stresses q_c measured for wide base tires are more sensitive to the actual loading conditions than to the tire inflation pressure. In case of the bias ply tire, a 100% tire load increase yields an increase of the q_c value of approximately 25% for a constant tire inflation pressure, while the increase is under 5% in the case of the radial but about 15% for wide base tire type. If the applied load is kept constant and the tire inflation pressure is increased only 50%, the average center tire contact stress q_c increases about 93% for the bias ply tire, and about 45% and 27% in the cases of the radial and the wide base tire, respectively. This proves a dominant influence of the actual tire inflation pressure p_i on the resulting average tire center contact stress q_c, as postulated earlier by several authors (e.g., *Groenendijk,* et al. *1997*, *Yap 1988*). However, for the bias ply and the wide base tires, the influence of the vertical tire loading is not negligible. Within the rated load and tire inflation ranges, the average tire center contact stresses q_c of the radial tire and the bias ply tire are approximately the same, but the corresponding value for the wide base tire is about 20% higher.

Figure 7 illustrates the development of the average tire edge contact stress q_e for the three tire types tested. This can be expressed as function of the applied vertical tire load F_z. The influence of the inflation pressure is negligible. The q_e values measured for radial tire type are most sensitive to the applied load. A 50% increase in the applied tire load produces an increase of the average contact stress at the tire edge of between 35 to 40%. This increase is between 27 to 35% and 12 to 17% for wide base tires and bias ply tires, respectively. However, in the rated load ranges of the tires, the average tire edge contact stress q_e of the radial tire is about 8% lower than the contact stress measured for the bias ply tire. Further, it is important to note that for the wide base tire, the edge contact stress at the rated load is in the same approximate range as for the bias ply tire type.

Maximum Tire Contact Stresses

In addition to the comprehensive analysis of the average vertical tire contact stress distributions obtained for each tire imprint, the ratios of the maximum (peak) stresses in the longitudinal (max. t_{zx}), lateral (max. t_{zy}) and vertical direction (max. s_{zz}) to the actual tire inflation pressure p_i were computed. This ratio is also called the Normalized Contact Pressure (NCP) (*Tielking, 1989*) and is considered to be useful to quantify peaks of the tire contact stresses measured. The results are given in the form of boxplots of the NCP as function of the tire inflation pressure p_i for the three different tire types (Figures 8 a–c).

For the bias ply tire, the measured lateral peak stresses t_{zy} have in average 29% and the longitudinal peak stresses t_{zx} in average 13% of the magnitude of the vertical stress s_{zz}. For the radial tire, the percentage ratio of the average lateral maximum contact stress t_{zy} is lower (23%) but higher for the longitudinal peak stress (18%). This is again caused by the higher stiffness of the tread zone in combination with a lower stiffness of the wall of the radial tire. As result of the width-to-length ratio of about 1 measured for the wide base tire imprints, the tire stiffness and therefore the values of the maximum contact stresses in the lateral and longitudinal direction is similar and both are in the range of about 19% of the vertical peak stresses. Regarding the maximum vertical stresses, the mean of the NCP ratios at the rated tire inflation pressure is between 1.7 to 1.9 for all three tire types, which compares well with similar findings from Yap (*1988*) and De Beer, *et al.* (*1997*).

Some general statistics about the measured *NCP* ratios for the peak stresses measured in each load direction (*n* – sample number, *m* – mean value, *s* – standard deviation, *min* – lowest ratio measured, *max* – highest ratio measured) together with the percentile values for a percentile of 5 up to 95% are given in Table 8 (p. 13).

Improved Assumptions to Model Vertical Tire Contact Stresses

Depending on which options a particular analytical pavement model offers for modeling the contact stress of the tire, the findings and regression analysis presented above can be utilized differently. The most common pavement analysis programs used allow only a limited number of either circular or rectangular uniformly distributed loads in the vertical direction.

If the tire/pavement contact stress is modeled by only one uniformly distributed circular load, Equation (1) may be used to obtain the relevant average vertical contact stress q as function of the applied vertical tire load F_z and the tire inflation pressure p_i. Hence, the load radius can be determined. In this case, higher levels of reliability are recommended. Enhancements might be achieved by imposing three circular loads to simulate tire center and tire edge loading. By means of the load distribution factor a calculated from Equation (3), both edge and center tire loads F_e and F_c, respectively, can then be computed from F_z and p_i as well as the average tire edge and tire center contact stresses p_c and p_e from Equation (4) and (5). Consequently, the load radius for the center and for both edge loads may be determined. To simulate the actual tire imprint, the center load circle should be situated in the center axis of the tire load and the two edge load circles at a distance $d = 0.4\ w$ of the (constant) width of the tire tread area (see Figure 9).

In the case of modeling tire/pavement contact area as a rectangle, the total width w is equal to the width of the tire tread area. Two rectangles simulate the edge and one the center load. The width of the rectangles is 20% and 60%, respectively, of the total width w. Their length can be determined from the average contact stresses of the tire edge and tire center zone calculated from Equations (4) and (5), and the center and edge load as function of a derived from Equation (3) (see Figure 9).

First comparison calculations with a finite element (FE) program computed for a 3D linear elastic multi-layer system show reasonable results and encourage the application of these more advanced load models in pavement design routines. However, as the effects on the primary response are fairly complex and their detailed description is out of the scope of this paper, further analyses are recommended in order to better quantify their consequences on pavement design.

These load models consider vertical tire contact stresses by using some rather simple approaches. However, as already discussed, all measurements display significant high longitudinal and transverse shear stresses at the tire/pavement interface even in the case of a free-rolling non-driven tire. The pattern observed for these shear stresses is influenced by many different parameters that consequently are not easy to quantify by (simple) regression functions. Hence, some attempts have been made to describe the longitudinal stress distribution by means of a sine function and the transverse stress distribution as a zigzag distribution (*Groenendijk,* et al. *1997*) but with rather poor regression results as acknowledged by the authors. It was therefore decided not to put further efforts into more refined modeling of these shear stresses, rather to transform the SIM measurement itself into a corresponding pattern of shear and normal stresses, which can then be read and processed by modern analytical pavement analysis programs.

STRESS-IN-MOTION ANALYSIS SOFTWARE

The objective of this software is to utilize the Stress in Motion (SIM) records available for different tire types, loading, and tire inflation pressure conditions to produce corresponding load models for analytical pavement design. This is achieved by transposing the row data recorded in the field with the VRSPTA device into a merely space related stress or load pattern that represents the optimized actual contact stress state at the tire/pavement interface and that can be processed by a pavement analysis program used for design calculations. Consequently, SIM measurements may be used to create easy-to-access load libraries of tire contact stress distributions for the more realistic analysis of pavement response near the surface.

The Stress in Motion (SIM) Analysis software developed runs in a Microsoft Windows environment and features the following options in the main menu:

- Transformation of Stress in Motion Records
- Statistics of SIM – Records
- Create Load Library
- Edit Stress in Motion Records.

In Figure 10 the structure of the SIM Analysis software with the different menu displays is illustrated. The different options of the program and their background are discussed in the following sections.

Transformation of Stress in Motion Records

The VRSPTA measures the vertical, transverse and longitudinal forces (loads) in real time with 20 instrumented pins in one line across the tire contact patch. When the rolling wheel is moved across the instrumented pins at a known measured speed, the actual forces are recorded with a fixed sample rate until the total tire contact area has passed over the surface of the VRSPTA. Typically, at wheel speeds of 0.3 m/s (“creep speed”) sampling rates of 150 Hz for a total of 256 samples were used for the measurements described in this paper. Therefore, the VRSPTA is a time and space based measuring system. Length intervals belonging to each sample of the 20 load records from the instrumented pins are obtained by dividing the measured wheel speed by the sampling rate. These length intervals are thus highly sensitive to the actual wheel speed at constant sample rates. In order to make use of these space and time dependent measurements for pavement analysis they have to be transformed into a space-only related stress pattern.

While the lateral distance dY of the forces measured with the VRSPTA is defined by the distance of 0.017 m between the instrumented pins, the longitudinal length interval dx is a function of sampling rate f and speed v of the passing wheel ($dx = v / f$). Hence, the value for dx always differs from one SIM record to the other. It is therefore advantageous to define a grid with a fixed distance between its nodes in both the longitudinal dX and lateral dY direction and to transpose the measured contact stresses into a pattern of corresponding stresses at this grid. The transformation problem is illustrated in Figure 11. Usually the node distance dX chosen is considerably larger than the length interval dx in order to reduce the number of node forces. For example, at a usual sampling rate f of 150 Hz and a passing speed of v = 0.3 m/s, the number of node forces would be about 3,200, if dX is chosen equal to dx = 0.02 m for a tire imprint with a length of 0.4 m and a width of 0.25 m.

By means of a transformation function, which provides the best fit to the data in the least squares sense, the measured forces are converted pin by pin to stresses at the corresponding node points of the defined grid. The actual stress at any given node, within each rectangular or area, is then defined by a bi-linear interpolation of the stresses at the four corners. In a final step, the calculated stresses at each node can be converted to node forces. This transformation method was adopted from a solution first used by *Weissman et al.* (*1997*) to derive the tire/pavement contact stress distribution of one SIM measurement for analytical pavement response calculations.

Since this transformation is sensitive to the position of the nodes of the grid relative to the actual position of the tire on the VRSPTA, which corresponds to a particular sample of stresses measured by the instrumented pins, a method was developed that optimizes the final position of the grid on the best fit to the resulting total vertical tire load calculated from both the SIM record and the transposed node forces. The final result is then stored in an output file, which contains a header, the node number in longitudinal and vertical directions, and the array of corresponding node stresses calculated.

For example, a grid with a square node distance of *dX* and *dY* = 0.017 m, the number of forces to model a tire imprint with the same geometry mentioned above (length = 0.4 m and width = 0.25 m) is reduced from about 3,200 to only 360. This is a number which most modern analytical pavement design programs are capable of handling.

In Figure 12, the plots of the 3D SIM records measured for a radial tire with an applied vertical force of 56 kN and a tire inflation pressure of 690 kPa are shown opposite the plots of corresponding stresses transformed by the SIM Analysis software to a grid with a square node distance of 0.017 m by 0.017 m. The different plots illustrate that the transformation function developed maintains the characteristic shape and image of the tire contact stresses actually measured and smoothes the results by filtering out most of the inherent noise from the data.

Creating a Load Library

After the SIM measurements are transformed at nodes of a rectangular grid and stored in a text file, the stress patterns of the tire imprint can then be utilized for pavement analysis. The different files may be combined to simulate any individual tire load group of single or dual tires by means of simple coordinate transformation. Subsequently, the created load group must be converted into the syntax of the input file of the pavement analysis program used.

Currently the SIM Analysis software offers two options: The translation of the transformed SIM measurements into a syntax that can either be processed by the Linear Elastic Analysis Program LEAP or the 3D Finite Element Program FEAP. LEAP is software of the Pavement Research Center (PRC) at UCB to analyze 3D multi layer elastic systems. It has no restrictions on the number of applied loads and system layers to model. FEAP is a 3D finite element analysis program developed by Prof. R. Taylor at the Department of Civil and Environmental Engineering at UCB. For the LEAP software, the contact stresses at each of the nodes are converted into a pattern of corresponding uniformly distributed circular loads. In the case of FEAP, the SIM measurements are used to specify force boundary conditions of an FE mesh. The SIM Analysis software creates an input file that defines a force distribution in the syntax of the FEAP program. Figure 13 gives an example for the 3D force pattern calculated from the contact stresses measured with the VRSPTA for a the same radial tire shown in Figure 12 (for demonstration purposes the signs of the vertical forces were changed).

For the generation of FEAP or LEAP load input files, the force units can be selected as well as the direction (lateral, longitudinal, vertical) of the measured tire contact stresses. Therefore, the effects of tire shear forces and vertical forces can be studied separately. As another important feature, the SIM Analysis software allows users to create load patterns of single or dual tires. The latter might be assembled by any combination of tires with different load and inflation pressures from available SIM measurements.

Statistics of SIM Records

This program module allows the user calculate different parameters of the tested tire from any SIM data file (see screen display in Figure 10). The selected parameters are computed for the chosen SIM record and written into a specified output file. The output file has a standard text format readable by most statistical analysis software products.

Editing the Stress-in-Motion Records

This file editor (see screen display in Figure 10) was included in the software in order to facilitate the handling of different SIM files and to visualize the SIM measurements in a 3D graph. However, the module to visualize the measurements has not been implemented yet.

CONCLUSIONS

Inflation pressure, load and tire type have a significant influence on the 3D contact stress distribution occurring between tire and pavement surface. By means of regression analysis, the different behaviors of the three tire types tested in this study could be quantified as functions of inflation pressure and load. The study verifies previous findings that the distribution of vertical contact stress develops significantly differently at the tire edge and tire center under different load and inflation pressure conditions. Since high contact stresses at the tire edge are considered to be one key factor in the development of such surface-related pavement distresses as rutting and

surface cracking, the concept described to determine vertical tire edge and center contact stresses might help to improve load models for pavement analysis. However, further studies are recommended to assess in detail the resulting effects.

With the Stress-In-Motion (SIM) analysis program an advanced tool has been developed to incorporate 3D tire contact stress distributions measured with the Vehicle–Road Surface Pressure Transducer Array (VRSPTA) System in pavement analysis and design methods. By means of the SIM software, load libraries based on the measured contact stresses of tires can be created in order to assemble different load groups that specify the characteristics of the complex contact stresses under truck tires, and that simulate different tire load and inflation pressure conditions. By introducing these improved loading assumptions into analytical pavement models, further research can be expected to yield a more complete understanding of stress distributions in pavement structures in the immediate vicinity of the tire. This in turn will contribute to fully understanding the mechanisms of pavement failure concentrated near the surface. These failure models are recognized as becoming the predominant distress problem for heavy duty roads, and should therefore be considered in proper design and performance prediction of pavements.

ACKNOWLEDGMENTS

The authors wish to thank the Max Kade Foundation for their award to Ronald Blab of a Post-Doctoral Research Exchange Grant to finance his research stay at the Pavement Research Center at the University of California, Berkeley.

REFERENCES

de Beer, M. (1994): *Measurements of tyre/pavement interface stresses under moving wheel loads*. Research Report DPVT 224 (Revised), Pavement Engineering Technology, Division of Roads and Transport Technology, CSIR, April 1994.

de Beer, M. (1995a): *Tyre/pavement interface stresses measured with the Vehicle – Road Surface Pressure Transducer Array (VRSPTA) system (i.e. "3-D Loadcell"); Part I: The VRSPTA system some technical details*. (Unpublished Confidential Technical Note I/P/11/95, Pavement Engineering Technology), Pretoria: Division of Roads and Transport Technology, CSIR, 1995.

de Beer, M. (1995b): *Tyre/pavement interface stresses measured with the Vehicle – Road Surface Pressure Transducer Array (VRSPTA) system (i.e. "3-D Loadcell"); Part II: Data analysis: vertical stress*. (Unpublished Confidential Technical Note I/P/11/95, Pavement Engineering Technology), Pretoria: Division of Roads and Transport Technology, CSIR, 1995.

de Beer, M. and Fisher, C.(1997): *Contact stresses of pneumatic tires measured with the Vehicle – Road Surface Pressure Transducer Array (VSPTA) system for the University of California at Berkeley (UCB) and the Nevada Automotive Test Center (NATAC)*. Restricted Report, Volume I and Volume II, University of California at Berkeley (UCB) and the Nevada Automotive Test Center (NATAC), June 1997.

Groenendijk, J.; Miradi, A.; Molenaar, A.A.A; Vogelzang, C.H.; Dohmen, L.J.M; Maagdenberg, A.M.; de Beer, M. (1997): Pavement Performance Modeling using LINTRACK. *Proceedings, 8th International Conference on Asphalt Pavements*, Vol. II, Seattle, WA, August 1997, pp.1505 –1526.

Tielking, J.T. (1989): Aircraft Tire / Pavement Pressure Distributions. *SAE Technical Paper Series*, 892351, Anaheim, CA, September 1989.

Weismann, S.L. and Sackman, J.L. (1997): *The Mechanics of Permanent Deformation in Asphalt – Aggregate Mixtures: A Guide to Laboratory Test Selection*. Symplectic Engineering Corporation, Albany, CA, December 1997.

Yap, P. (1988): *A Comparative Study of the Effects of Truck Tire Types on Road Contact Pressures*. Vehicle Pavement Interaction – where the truck meets the road, SP – 765, Society of Automotive Engineers, Inc., Warrendale, PA, November 1988.

TABLES AND FIGURES

TABLE 1 Test Matrix of the 425/65R22.5 Wide Based Tire

Load [a] [kN]	Tire Inflation Pressure[b] [kPa] 500	620	690	700	760
26	*X*	*X*	*X*	*X*	-
46	*X*	*X*	*X*	*X*	-
49	-	-	-	*X*	-
56	*X*	*X*	*X*	*X*	*X*
66	*X*	*X*	*X*	*X*	-
86	-	*X*	*X*	*X*	-
106	-	*X*	*X*	*X*	-

[a] 1 kN = 224.7 lbf

[b] 1 kPa = 0.145 psi

TABLE 2 Test Matrix of the 10.00-20 Bias and 11R22.5 Radial Tires (tested as singles)

Load [a] [kN]	Tire Inflation Pressure[b] [kPa] 220	420	520	620	690	720	820	920
26	*X*	*X*	*X*	*X*	*X*	*X*	*X*	*X*
31	*X*	*X*	*X*	*X*	*X*	*X*	*X*	*X*
36	*X*	*X*	*X*	*X*	*X*	*X*	*X*	*X*
41	-	*X*	*X*	*X*	*X*	*X*	*X*	*X*
46	-	*X*	*X*	*X*	*X*	*X*	*X*	*X*
51	-	-	*X*	*X*	*X*	*X*	*X*	*X*
56	-	-	*X*	*X*	*X*	*X*	*X*	*X*

[a] 1 kN = 224.7 lbf

[b] 1 kPa = 0.145 psi

TABLE 3 Statistics of Measured Tire Width

Tire Type	Load Range[a]	Inflation	Size	Mean[c]	Std. Error[c]	Std. Dev.[c]
Bias Ply Tire	26 - 56	420 - 920	141	0.211	0.0013	0.015
Radial Tire	26 - 56	420 - 920	141	0.203	0.0009	0.011
Wide Base Tire	26 -106	500 - 760	72	0.320	0.0014	0.012

[a] 1 kN = 224.7 lbf

[b] 1 kPa = 0.145 psi

[c] 1 m = 3.279 ft

TABLE 4 Regression Constants and Statistics for Average Tire Contact Stress

Tire Type	Regression Range Load [a] [kN]	Regression Range Inflation [b] [kPa]	Regression Constants and Statistics k_1 [b] [kPa]	k_2	k_2	R^2	Std. Error [b] [kPa]
			50% Reliability				
Bias Ply	26 - 56	220 - 920	142.46	0.335	4.359	0.934	22.1
Radial	26 - 56	220 - 920	188.22	0.281	4.834	0.849	33.2
Wide Base	26 -106	500 - 760	119.50	0.334	3.509	0.776	61.7
			80% Reliability				
Bias Ply	26 - 56	220 - 920	150.066	0.343	4.516		
Radial	26 - 56	220 - 920	199.543	0.294	5.068		
Wide Base	26 -106	500 - 760	149.679	0.370	3.767		
			90% Reliability				
Bias Ply	26 - 56	220 - 920	154.041	0.348	4.599		
Radial	26 - 56	220 - 920	205.462	0.300	5.190		
Wide Base	26 -106	500 - 760	165.454	0.389	3.901		
			95% Reliability				
Bias Ply	26 - 56	220 - 920	157.325	0.351	4.667		
Radial	26 - 56	220 - 920	210.350	0.306	5.291		
Wide Base	26 -106	500 - 760	178.481	0.405	4.012		

[a] 1 kN = 224.7 lbf

[b] 1 kPa = 0.145 psi

TABLE 5 Regression Constants and Statistics for Bias Ply Tires

Parameter	Regression Constants and Statistics Estimate	Std. Error	95% Confidence Interval Lower	Upper
	$\alpha = f(p_i, F_z)$ - R^2 = 0.638			
k_1	$8.898\ 10^{-2}$	$7.394\ 10^{-2}$	$-5.718\ 10^{-2}$	0.235
k_2	$1.139\ 10^{-3}$	$8.323\ 10^{-5}$	$9.748\ 10^{-4}$	$1.304\ 10^{-3}$
k_3	$6.983\ 10^{-3}$	$1.641\ 10^{-3}$	$3.740\ 10^{-3}$	$1.023\ 10^{-2}$
	q_c [a] [kPa] = $f(p_i, F_z)$ - R^2 = 0.979			
k_1 [a] [kPa]	-15.588	7.048	-29.520	-1.657
k_2	0.541	0.008	0.525	0.557
k_3	4.179	0.156	3.870	4.488
	q_e [a] [kPa] = $f(F_z)$ - R^2 = 0.762			
k_1 [a] [kPa]	227.647	48.643	131.495	323.799
k_2	12.317	2.536	7.305	17.329
k_3	-0.076	0.032	-0.139	-0.0137

[a] 1 kPa = 0.145 psi

TABLE 6 Regression Constants and Statistics for Radial Tires

Parameter	Regression Constants and Statistics			
	Estimate	Std. Error	95% Confidence Interval Lower	Upper
	$\alpha = f(p_i, F_z)$ - $R^2 = 0.722$			
k_1	0.840	0.051	0.740	0.940
k_2	$9.493\ 10^{-4}$	$5.609\ 10^{-5}$	$8.385\ 10^{-4}$	$1.060\ 10^{-3}$
k_3	$-1.336\ 10^{-2}$	$1.043\ 10^{-3}$	$-1.542\ 10^{-2}$	$-1.130\ 10^{-2}$
	q_c [a] [kPa] = $f(p_i, F_z)$ - $R^2 = 0.727$			
k_1 [a] [kPa]	190.230	22.241	146.272	234.187
k_2	0.438	0.023	0.392	0.483
k_3	0.864	0.477	-0.079	1.807
	q_e [a] [kPa] = $f(F_z)$ - $R^2 = 0.894$			
k_1 [a] [kPa]	17.615	60.862	-102.676	137.907
k_2	19.189	3.197	12.870	25.508
k_3	-0.087	0.040	-0.167	-.007

[a] 1 kPa = 0.145 psi

TABLE 7 Regression Constants and Statistics for Wide Base Tires

Parameter	Regression Constants and Statistics			
	Estimate	Std. Error	95% Confidence Interval Lower	Upper
	$\alpha = f(p_i, F_z)$ - $R^2 = 0.741$			
k_1	2.292	0.213	1.868	2.716
k_2	$1.317\ 10^{-3}$	$2.553\ 10^{-4}$	$8.077\ 10^{-4}$	$1.825\ 10^{-3}$
k_3	$-2.416\ 10^{-2}$	$1.844\ 10^{-3}$	$-2.782\ 10^{-2}$	$-2.051\ 10^{-2}$
	q_c [a] [kPa] = $f(p_i, F_z)$ - $R^2 = 0.671$			
k_1 [a] [kPa]	119.380	42.799	34.062	204.698
k_2	0.450	0.051	0.349	0.552
k_3	2.318	0.351	1.618	3.019
	q_e [a] [kPa] = $f(F_z)$ - $R^2 = 0.919$			
k_1 [a] [kPa]	109.646	33.154	43.556	175.737
k_2	8.657	1.051	6.562	10.752
k_3	-0.015	0.007	-0.030	0.0003

[a] 1 kPa = 0.145 psi

TABLE 8 Statistics of Maximum Contact Stresses

Ratio	Descriptive Statistics					Percentile				
	n	m	s	min	max	5%	25%	50%	75%	95%
					Bias Ply Tire					
max σ_{zx} / P_I	150	.267	.207	.09	1.14	.114	.160	.192	.294	.899
max σ_{zy} / P_I	150	.590	.324	.17	1.78	.258	.386	.488	.730	1.418
max σ_{zz} / P_I	150	1.871	.709	.99	4.10	1.059	1.404	1.677	2.200	3.869
					Radial Tire					
max σ_{zx} / P_I	150	.339	.198	.12	1.07	.160	.210	.279	.398	.919
max σ_{zy} / P_I	150	.414	.174	.20	1.08	.259	.295	.364	.450	.830
max σ_{zz} / P_I	150	1.805	.642	1.15	4.66	1.261	1.404	1.578	2.018	3.048
					Wide Base Tire					
max σ_{zx} / P_I	72	.339	.126	.10	.64	.153	.240	.331	.420	.558
max σ_{zy} / P_I	72	.318	.063	.13	.45	.192	.280	.322	.354	.430
max σ_{zz} / P_I	72	1.740	.232	1.40	2.36	1.474	1.581	1.679	1.822	2.282

FIGURE 1: Top View of the Vehicle-Road Surface Pressure Transducer Array (*De Beer et al. 1997*)

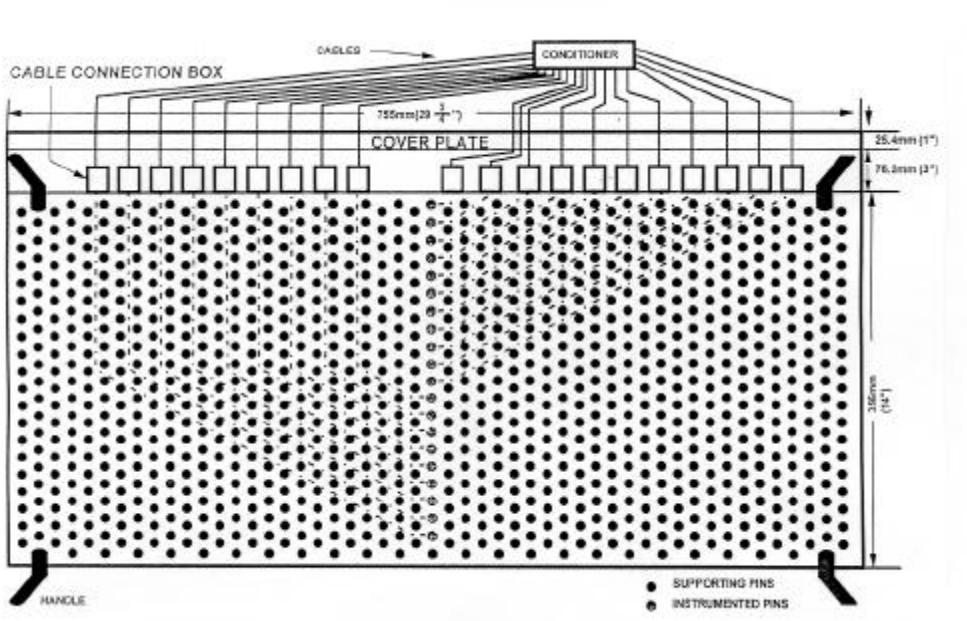

FIGURE 2 Mean Ratio Tire Width to Length as a Function of Load

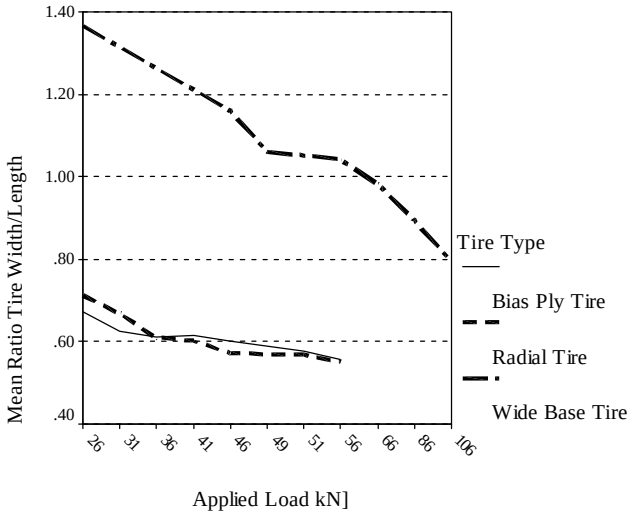

FIGURE 3 Mean Ratio Tire Width to Length as a Function of Inflation Pressure

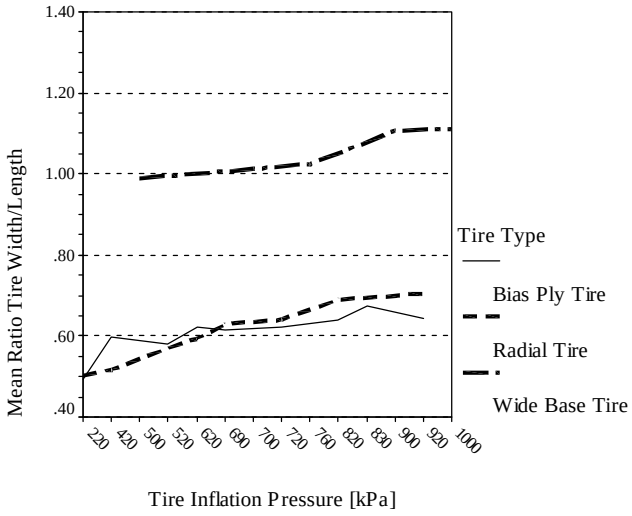

FIGURE 4 Ratio of Average Contact Pressure to Inflation Pressure for different Levels of Inflation Pressure

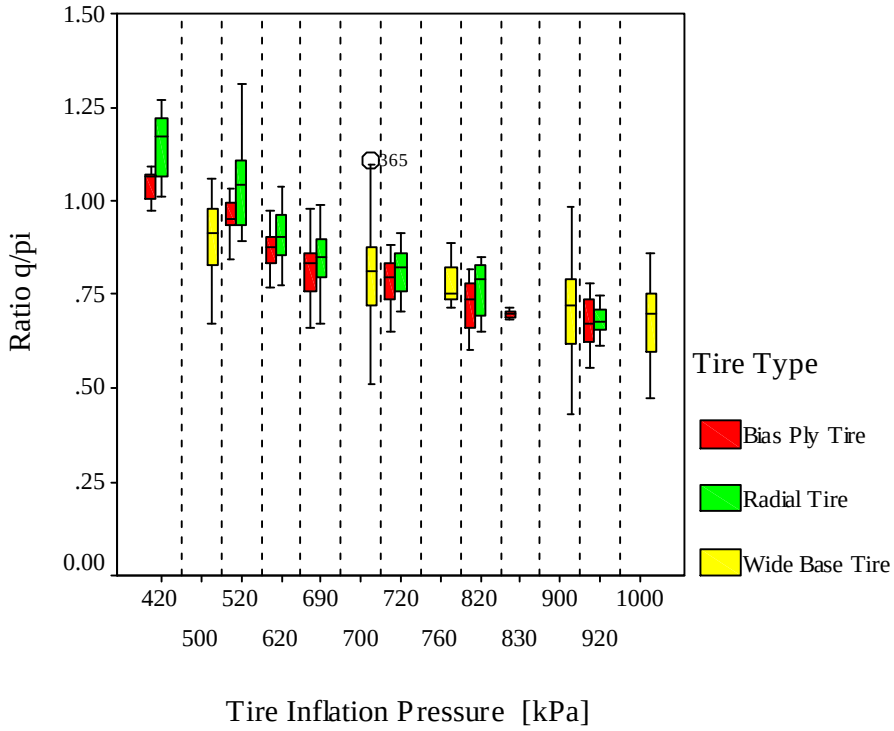

FIGURE 5 Load Distribution Factor a as Function of Tire Load and Inflation Pressure

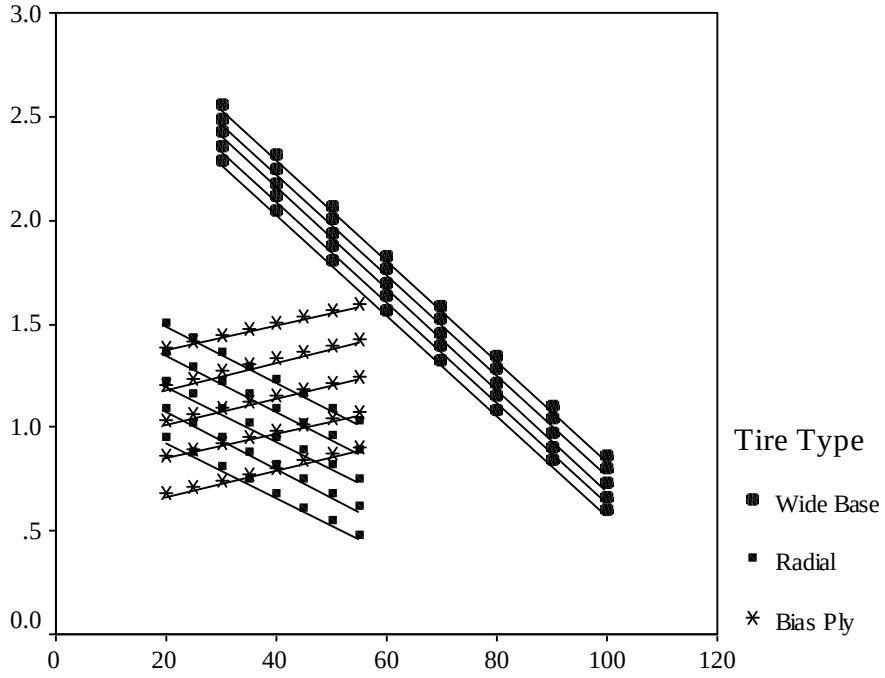

FIGURE 6 Average Tire Center Contact Stress as Function of Load and Inflation Pressure

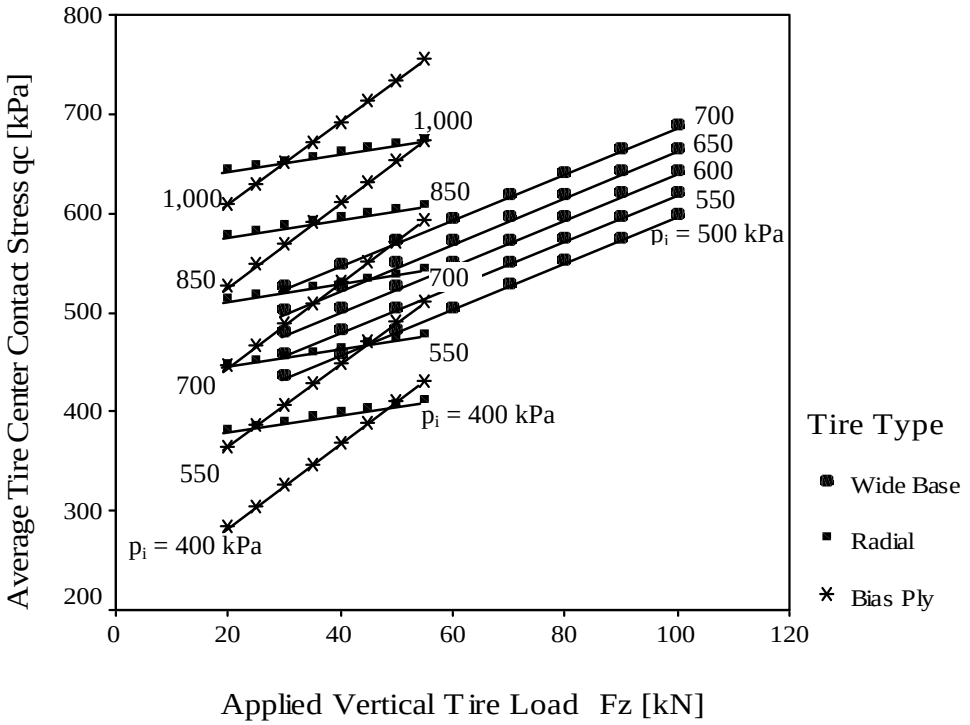

FIGURE 7 Average Tire Edge Contact Stress as Function of Load

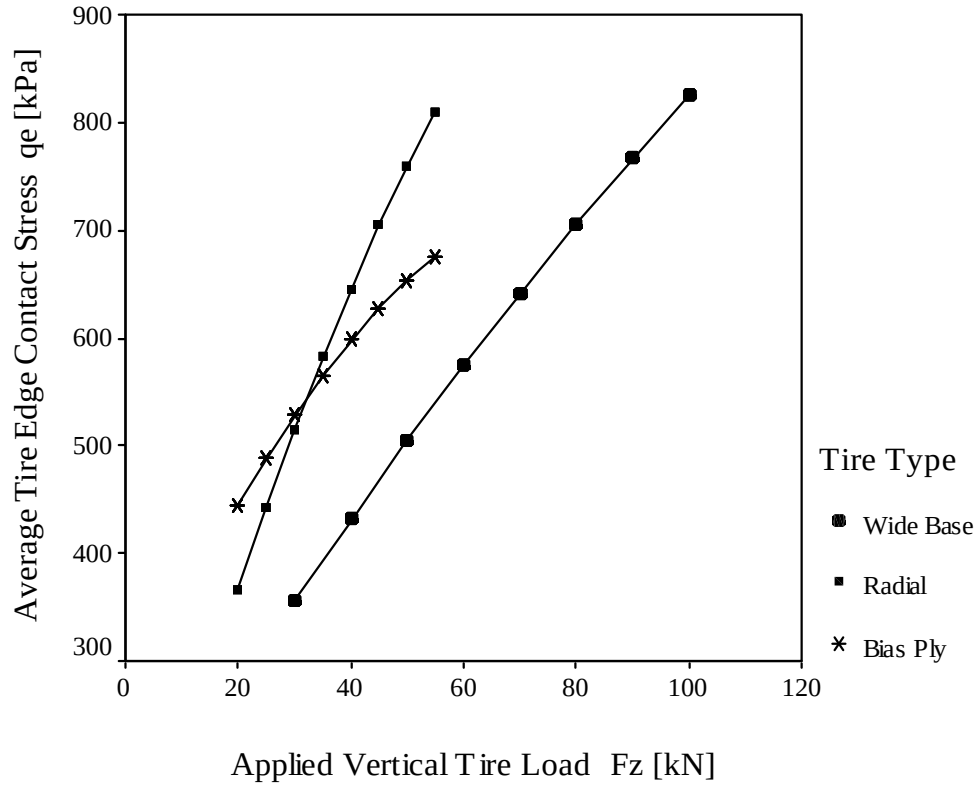

FIGURE 8 Normalized Contact Pressure NCP for Different Levels of Inflation Pressure

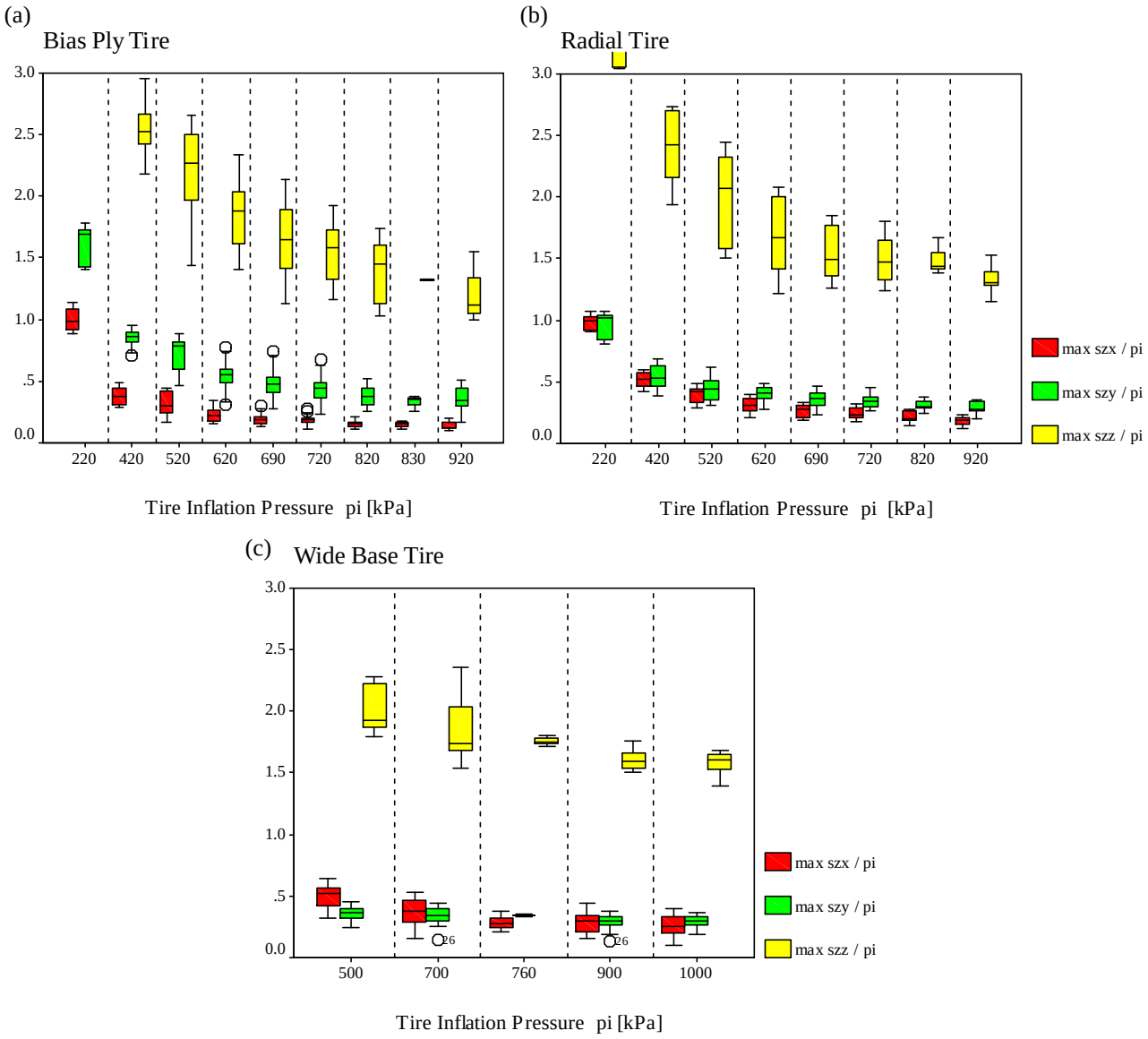

FIGURE 9 Load Configuration to Simulate Tire Edge and Center Load with Uniformly Distributed Loads of Circular or Rectangular Shape

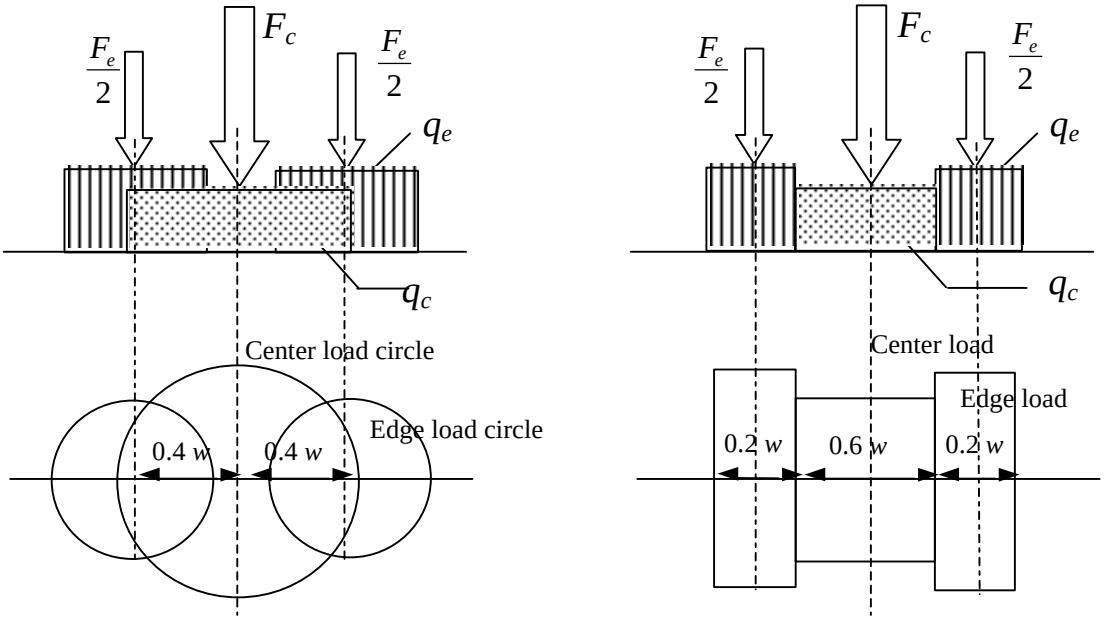

FIGURE 10 Structure of the Stress In Motion Analysis Program

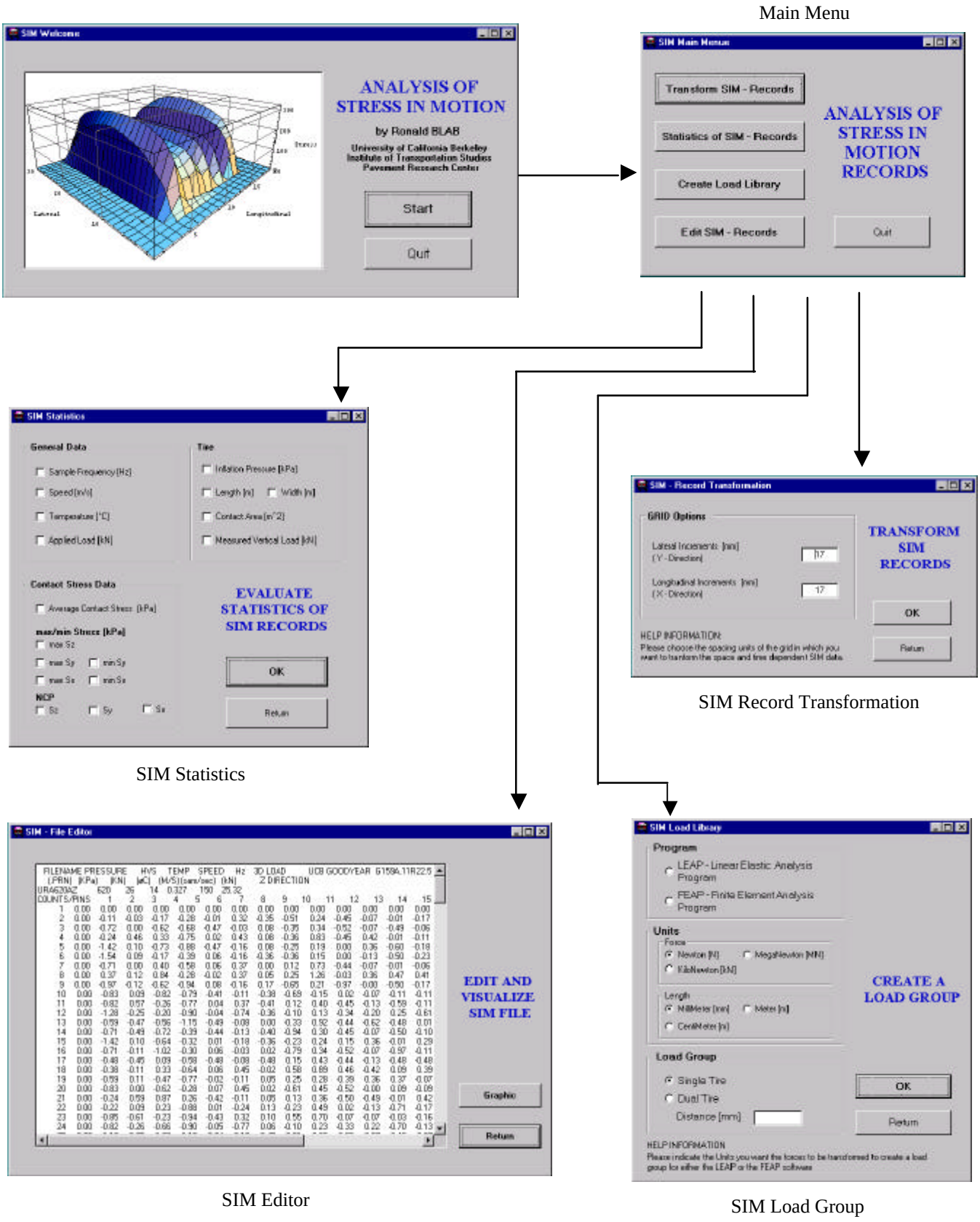

FIGURE 11 Transformation of SIM Measurements

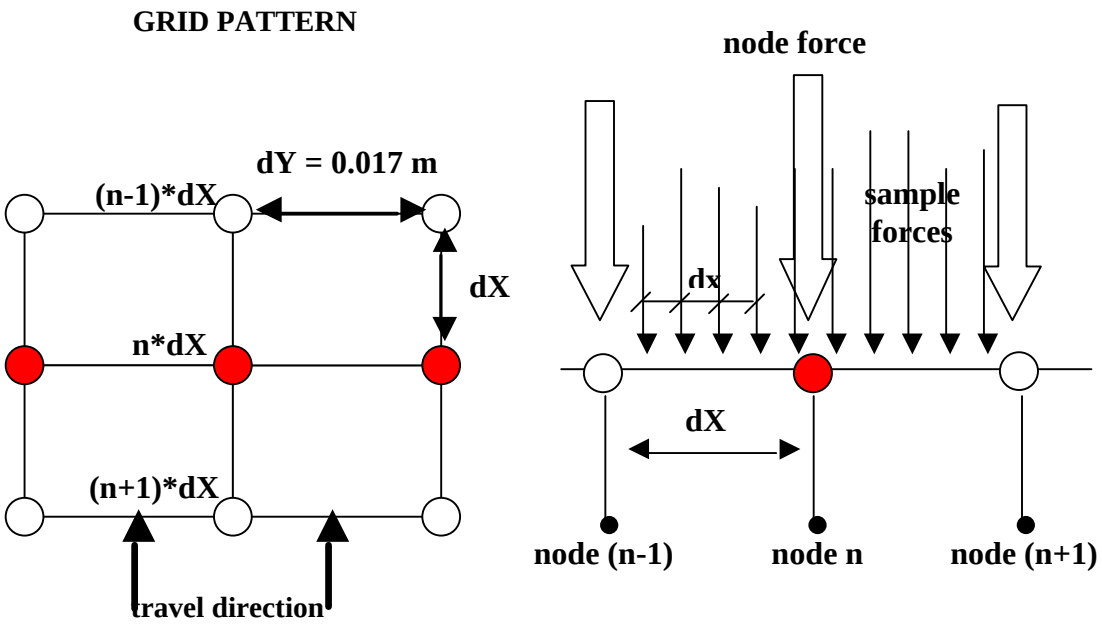

FIGURE 12 Measured and Transformed 3D – SIM Data from a Radial Tire

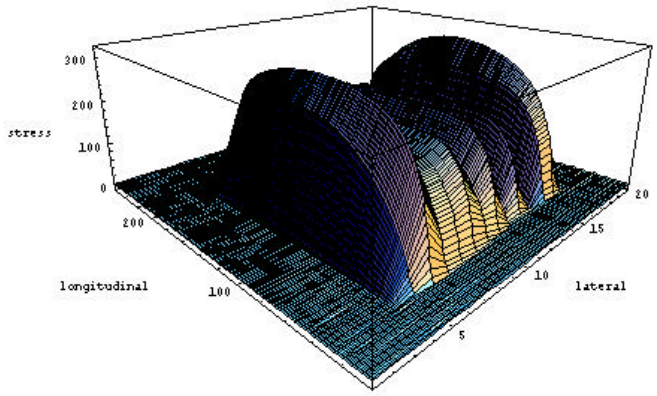

Z – direction: vertical stresses (measured)

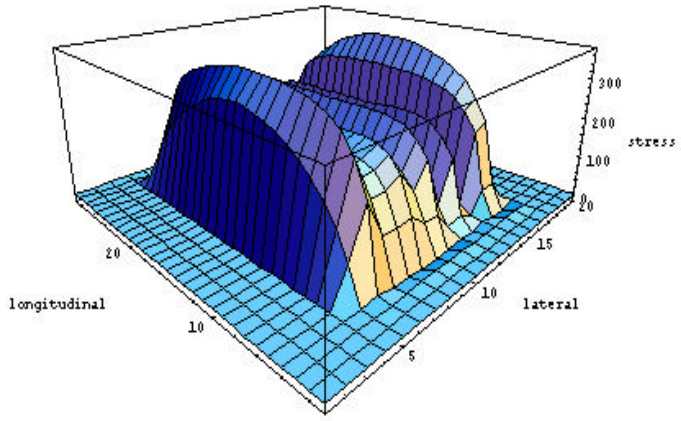

vertical stresses (transformed)

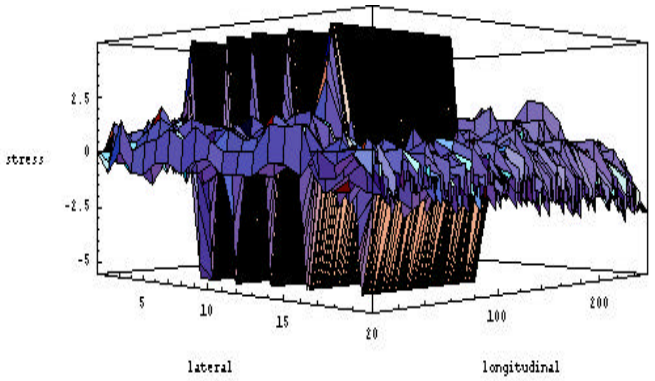

Y – direction: lateral stresses (measured)

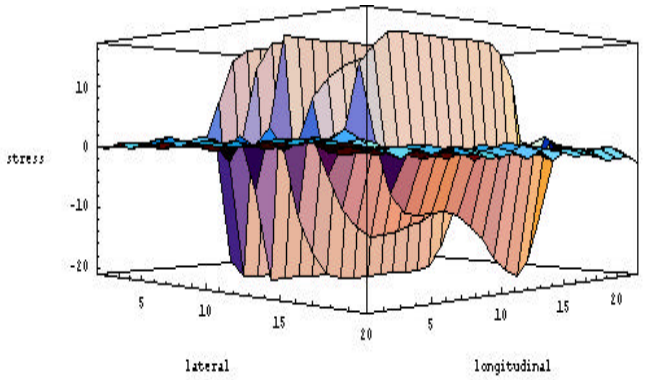

lateral stresses (transformed)

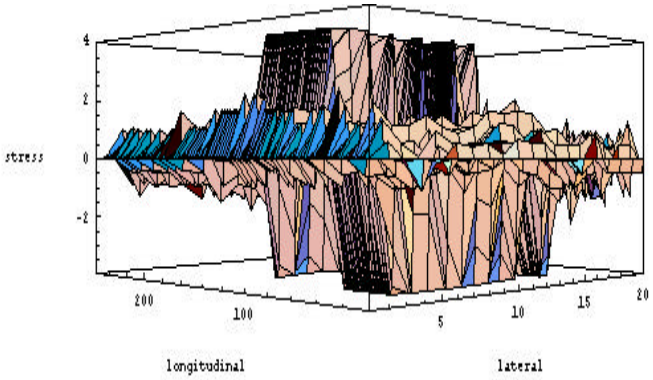

X – direction: longitudinal stresses (measured)

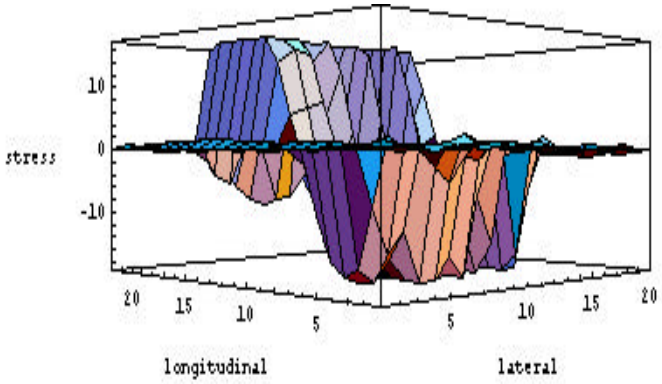

longitudinal stresses (transformed)

FIGURE 13 Force Pattern of the Contact Stresses measured with the VRSPTA of a Radial Tire in a FE Mesh

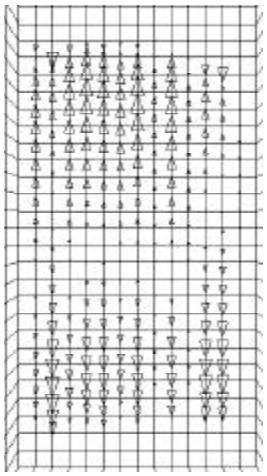

(a) longitudinal

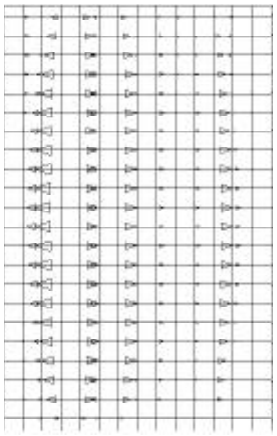

(b) transverse

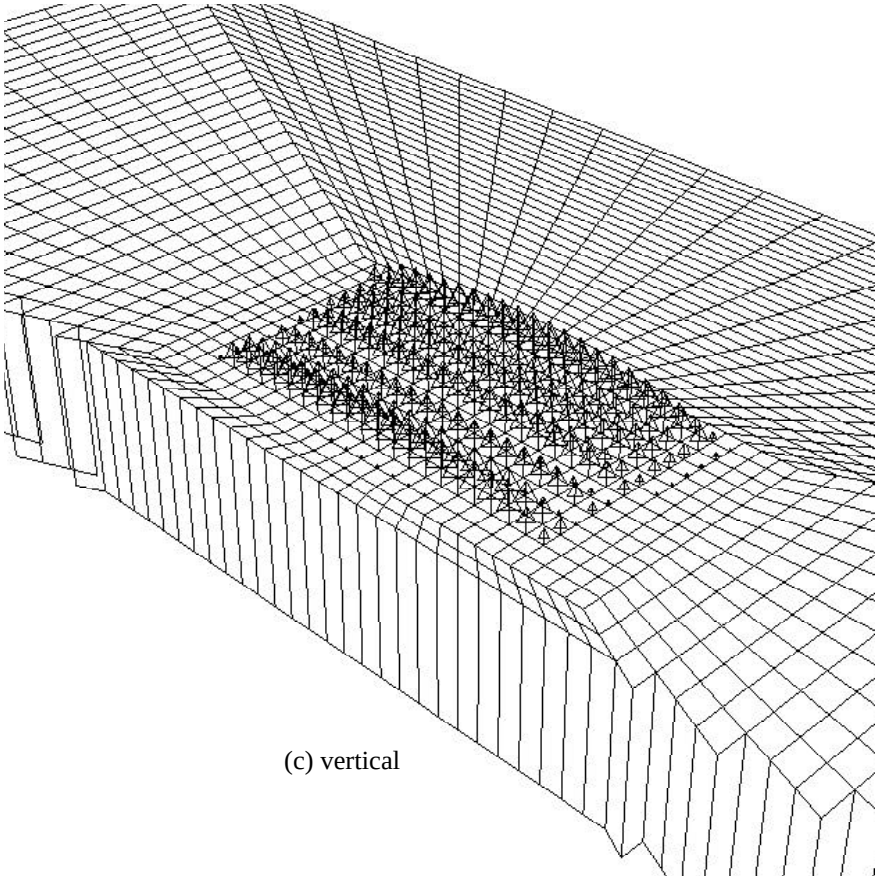

(c) vertical